Spatial transcriptomic analysis of cryosectioned tissue samples with Geo-seq

Jun Chen[1,2,6], Shengbao Suo[3,4,6], Patrick PL Tam[5], Jing-Dong J Han[3], Guangdun Peng[1] & Naihe Jing[1]

[1]State Key Laboratory of Cell Biology, Shanghai Institute of Biochemistry and Cell Biology, Chinese Academy of Sciences, Shanghai, China. [2]Department of Genetics and Cell Biology, College of Life Sciences, Nankai University, Tianjin, China. [3]Key Laboratory of Computational Biology, CAS Center for Excellence in Molecular Cell Science, Collaborative Innovation Center for Genetics and Developmental Biology, Chinese Academy of Sciences–Max Planck Partner Institute for Computational Biology, Shanghai Institutes for Biological Sciences, Chinese Academy of Sciences, Shanghai, China. [4]University of Chinese Academy of Sciences, Beijing, China. [5]Embryology Unit, Children's Medical Research Institute and School of Medical Sciences, Sydney Medical School, University of Sydney, Sydney, Australia. [6]These authors contributed equally to this work. Correspondence should be addressed to J.-D.J.H. (jackie.jdhan@gmail.com), G.P. (gdpeng@sibcb.ac.cn) or N.J. (njing@sibcb.ac.cn).

Published online 16 February 2017; corrected after print 13 April 2017; doi:10.1038/nprot.2017.003

Conventional gene expression studies analyze multiple cells simultaneously or single cells, for which the exact *in vivo* or *in situ* position is unknown. Although cellular heterogeneity can be discerned when analyzing single cells, any spatially defined attributes that underpin the heterogeneous nature of the cells cannot be identified. Here, we describe how to use geographical position sequencing (Geo-seq), a method that combines laser capture microdissection (LCM) and single-cell RNA-seq technology. The combination of these two methods enables the elucidation of cellular heterogeneity and spatial variance simultaneously. The Geo-seq protocol allows the profiling of transcriptome information from only a small number cells and retains their native spatial information. This protocol has wide potential applications to address biological and pathological questions of cellular properties such as prospective cell fates, biological function and the gene regulatory network. Geo-seq has been applied to investigate the spatial transcriptome of mouse early embryo, mouse brain, and pathological liver and sperm tissues. The entire protocol from tissue collection and microdissection to sequencing requires ~5 d, Data analysis takes another 1 or 2 weeks, depending on the amount of data and the speed of the processor.

INTRODUCTION

Environmental factors and the cellular niche influence cell identities during embryonic development, stem cell maintenance and differentiation, as well as tumorigenesis. Cells at different locations in a biological structure may receive a different quality or intensity of signaling pathway activity, which may result in the acquisition of spatially dependent cellular properties and fates. In contrast to *in vitro* cultured cells, the microenvironments of cells *in vivo* are dynamically and inherently heterogeneous, even within an apparently homogeneous setting. Therefore, when analyzing cellular properties such as the transcriptome of a cell, it is essential to study the spatially resolved attributes of a specific cell in its natural setting. Achieving this objective requires the application of a protocol to analyze the transcriptome of individual or a small group of cells from which their spatial information can be retrieved.

In recent years, transcriptome analysis for single cells or low-input RNA has been developed, and this has revolutionized the investigation of the heterogeneity and biological events in individual cells or cell populations. The application of such single-cell analysis has greatly facilitated experimental studies in oncology, cancer diagnosis[1,2], cellular immunity[3], stem cell properties[4,5] and developmental processes[6–9]. Many single-cell RNA-seq strategies with different strengths and efficacies have been developed[10]—e.g., Tang's protocol[11,12], CEL-seq[13], STRT[14] and the Smart-seq protocol[15–17]. A detailed comparison of these technologies has been done elsewhere[10,18,19].

A critical prerequisite for single-cell study is to efficiently harvest single cells of interest from tissues or a cell population. A variety of methods, such as cell sorting, manual picking (by micropipetting or mouth pipetting) and microfluidic separation, have been devised. Generally, these methods rely heavily on the mechanical or enzymatic dissociation of cell clumps or tissues into single-cell suspensions; therefore, any positional information of the cells is lost. Instead of deconstructing tissues into single cells, LCM enables precise capture of targeted cells, or even single cells, while retaining the structural (e.g., topographical anatomy, tissue histology and cellular morphology) and spatial information[20,21]. Thus, LCM is a spatially resolved strategy of cell harvesting. Studies of LCM-based transcriptome analysis have been performed successfully[22–27]. However, these studies required the collection of hundreds to thousands of cells, and only a limited set of genes were profiled. It is necessary to conduct a genome-wide omics analysis to interrogate the heterogeneity of cells in small samples or single cells with a low cellular-material (e.g., DNA and RNA) input and to render the data in a high-resolution 3D context. Here we provide details of a methodology (Geo-seq) that combines the technologies of LCM and single-cell RNA-seq to permit the study of the transcriptome of a small sample with as few as ten cells from defined geographical locations. With the accompanying spatial information, a 3D transcriptome atlas can be built up by Geo-seq to display the transcriptome spatially and quantitatively. A unique adjunct utility of Geo-seq is the ability to computationally retrieve the positional address of randomly collected single cells from stage-matched tissues by a zip-code mapping protocol, so that the functional attributes of each cell can be characterized against those of the cell population in which it resides. We have used Geo-seq to establish a 3D transcriptome atlas of a mid-gastrulation mouse embryo and mapped the individual single epiblast cells back to the *in vivo* embryonic position with a high accuracy[28]. Geo-seq has also been applied to delineate the cell identities of developing mouse brains, study the pathological status of human sperm and perform the functional characterization of mouse hepatocyte cells (data not shown).

Development of the protocol

Geo-seq is built on LCM[27] and single-cell RNA-seq technologies[16]. The most challenging task was to bridge these two technologies. In the Geo-seq protocol, we have optimized the LCM

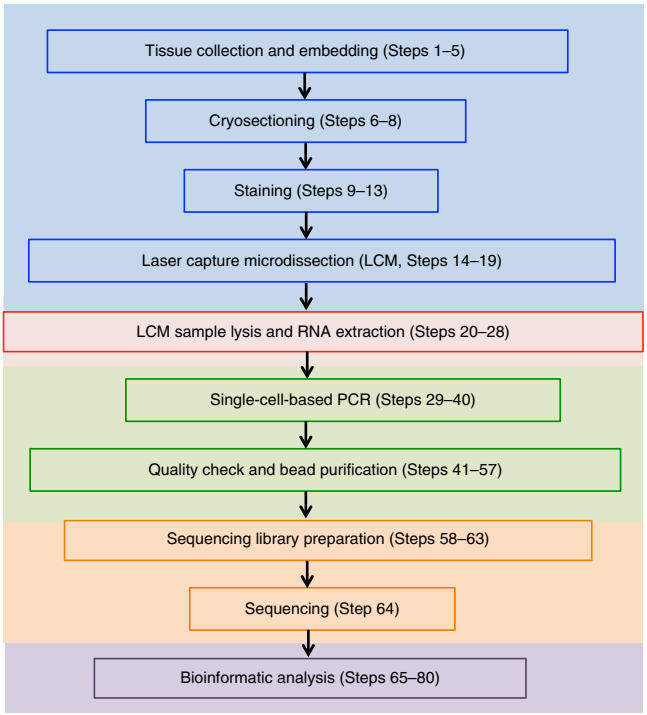

Figure 1 | Geo-seq workflow. After collection, the tissues are embedded in OCT medium and cryosectioned. Cells of interest are harvested by LCM after staining. Then the captured cells are lysed and the RNA is extracted. Single-cell PCR is performed to reverse-transcribe and amplify the purified RNA. The cDNA is used to construct the sequencing library, which is then sequenced. Geo-seq data are analyzed in customized bioinformatics pipelines.

procedure for preservation of cell morphology and RNA quality, as well as optimizing the method for sample lysis and the RNA yield to achieve robust technical performance. Furthermore, we modified the Smart-seq2 single-cell RNA-seq protocol to ensure its compatibility with LCM samples. Finally, we developed bioinformatics pipelines to analyze the Geo-seq data, render the data set into spatial gene expression profiles and enable the retrieval of positional address of the cells.

Overview of the procedure

The Geo-seq workflow is shown in **Figure 1**. Briefly, samples are collected and embedded in optimum cutting temperature (OCT) compound, followed by cryosectioning and staining. Cells of interest are harvested by LCM. During this relatively long processing time, it is critical to preserve the RNA quality of the LCM samples. Cells are lysed for the first cDNA synthesis, and a modified Smart2-seq protocol is performed to amplify the cDNA[16]. cDNAs that pass quality control are then used to construct the library for next-generation sequencing. Bear in mind that the mild lysis buffer used in single-cell RNA-seq must be modified for complex LCM samples. The procedure has been optimized for each step: tissue collection, cell lysis, RNA isolation and single-cell-based PCR amplification. Finally, downstream of RNA-seq, bioinformatics pipelines have been developed for visualizing the Geo-seq data in a 3D reconstruction or a 2D corn plot[28], and for identifying zip-code genes for mapping cell populations or single cells to specific locations in the embryos.

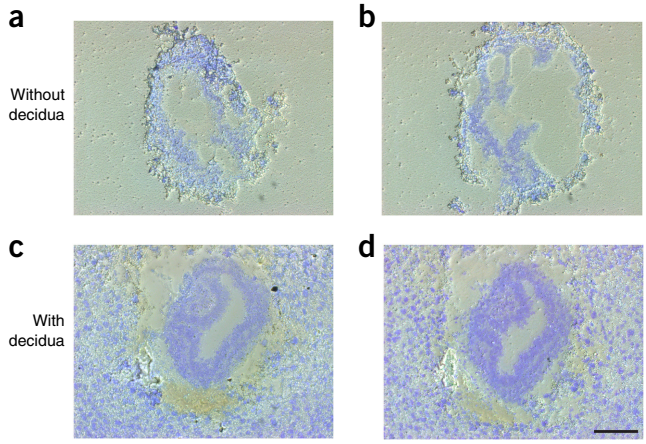

Figure 2 | Inclusion of the decidual tissue improves tissue integrity of the embryo cryosections. (**a**–**d**) Sections of specimens without decidua (**a**,**b**) and with decidua (**c**,**d**). Sections were stained with 1% (wt/vol) cresyl violet. Scale bar, 50 μm.

Experimental design

Tissue collection and embedding. The first stage of Geo-seq is to harvest fresh tissues for LCM and embedding. We have generated highly reproducible data from mouse embryo, mouse developing brain, mouse liver tissues and human germ cells; therefore, this protocol should be adapted to a variety of tissue types. To achieve optimal results, tissues should be isolated expeditiously, and best-practice preparation and handling of RNA samples is essential. For example, all the reagents should be RNase-free and all the instruments should be treated with RNase-removing reagents such as RNase-Zap. The tissue is washed by PBS, embedded in OCT compound with precise positioning and snap-frozen in liquid nitrogen or dry ice. After the OCT is completely frozen, the tissue can be stored at −80 °C for as long as 6 weeks without detectable RNA degradation.

Laser microdissection is an image-based technology. Well-preserved morphology of the specimen is vital for the capture. In the example study reported here, we focused on a mouse embryo at the gastrulation stage, which is inherently fragile. Preservation of the morphology of cryosections is best achieved by preparing the embryo sections together with the surrounding decidual tissue (**Fig. 2c**,**d**). The quality of the specimens is clearly superior to those from embryos without decidua (**Fig. 2a**,**b**), suggesting that the decidual tissues provide mechanical support.

A number of fixation methods are available for LCM treatment[29–31]. Although morphology is preserved better by fixation in formalin or 4% (wt/vol) paraformaldehyde (PFA), the quality and the yield of RNA are substantially compromised (**Fig. 3**), as also observed previously[30,32]. We adopted a fixation method involving serial ethanol dehydration to preserve both morphology and RNA quality.

Staining of the cryosection. Before microdissection, it is necessary to stain the cryosection for better visualization[33,34]. Staining with cresyl violet, H&E or Nuclear Fast Red is adequate to reveal sufficient anatomical detail of the sections for guiding LCM (**Fig. 4**, **Supplementary Methods**). However, substantial RNA degradation was observed when aqueous staining solutions (such as H&E)

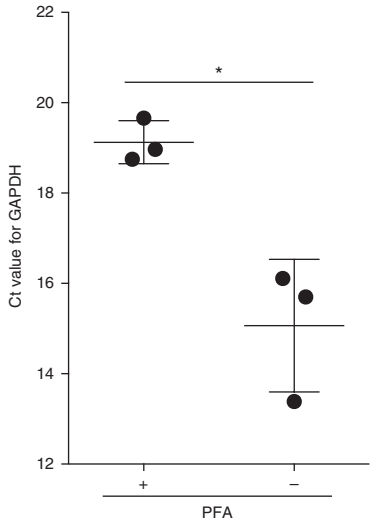

Figure 3 | PFA fixation decreases RNA quality severely. Gastrula-stage mouse embryos were fixed with PFA or unfixed, and RNA was extracted and reverse-transcribed. A lower level of a housekeeping gene (*GAPDH*) was detected (higher Ct value) in the PFA-fixed sample by real-time PCR, reflecting a poorer yield of RNA. $*P < 0.05$; three independent experiments were performed. Ct, cycle threshold.

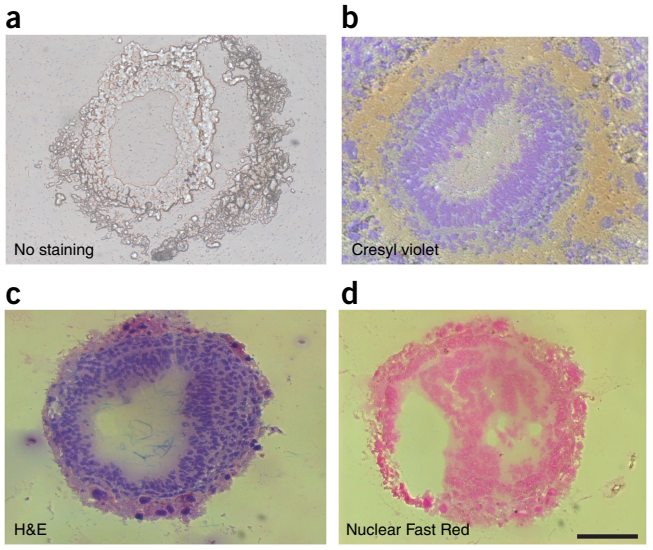

Figure 4 | Comparison of different staining methods. (**a**–**d**) Cryosections of gastrula-stage mouse embryo that were unstained (**a**) and stained with cresyl violet (**b**), H&E (**c**) and Nuclear Fast Red (**d**). Scale bar, 50 μm.

were used, whereas cresyl violet staining prepared in ethanol was adequate for maintaining the integrity of the RNA for up to 2 h[35]. Therefore, we recommend that cresyl violet staining be applied in Geo-seq.

Laser microdissection. The procedure for laser microdissection recommended by the manufacturer for RNA application should be strictly followed and a dedicated instrument in a confined space should be used to avoid contamination of experimental materials. The laser microdissection should be done within the shortest time possible. The parameters for LCM should be set at the lowest energy that can effectively dissect the samples. The methods for continuous and precise capture using the specific LCM platforms should be in place before collection. After cryosection, most LCM cells are not intact. Nevertheless, at least ten cells can be assayed.

Lysis and RNA isolation. After collection by LCM, the samples are lysed and single-cell-based PCR is performed. The lysis buffer for single-cell PCR is usually <5 μl and contains a solvent such as 0.45% (vol/vol) NP40 (ref. 12) or 0.1% (vol/vol) Triton X-100 (ref. 16), which are mild lysis detergents for a small-volume use. However, these lysis conditions are inadequate for releasing the RNA from LCM samples. Moreover, at least 10 μl of lysis buffer are required[23] to completely lyse LCM samples, which is not compatible with single-cell RNA-seq. Therefore, the lysis methodology is key to combining laser microdissection with single-cell PCR.

Guanidine isothiocyanate (GuSCN) is an effective protein denaturant for degrading endogenous ribonucleases and releasing RNA in a single step[36]. A previous study showed that low concentrations of guanidine isothiocyanate can be used to lyse single cells and followed by RT-PCR without purification[37]. However, lysis of the LCM sample with a small volume of GuSCN solution (5 μl) at low concentrations (0.05 M or 0.5 M) is insufficient for obtaining enough RNA molecules (**Fig. 5**). We reasoned that the small volume of low-concentration GuSCN might not thoroughly lyse LCM samples, and any residual GuSCN may adversely affect mRNA reverse transcription and cDNA amplification in the one-tube reaction. To overcome this barrier, we lysed LCM samples with 50 μl of GuSCN solution at a higher concentration (4 M) and performed ethanol precipitation to remove GuSCN and concentrate the RNA molecules. As a result, the outcome of single-cell-based qPCR using precipitated RNA was greatly improved (indicated by GAPDH expression; **Fig. 5**), and it produced a better yield than the commercial LCM RNA isolation kit (i.e., Arcturus Picopure RNA Isolation Kit).

Single-cell-based PCR and purification. RNA pellets are dissolved in the single-cell lysis solution and reverse-transcribed and amplified with a single-cell PCR technique. PCR amplification should be performed in a special-purpose lab that houses essential equipment such as a refrigerator, centrifuges, racks, lab coats, pipettes, tubes, pipette tips, reagent containers and so on. Among the many single-cell RNA-seq methods, Smart-seq2 was chosen because it can achieve full-length cDNA synthesis with a low PCR bias in a short time period[16,38]. However, Geo-seq is also compatible with common single-cell RNA-seq technologies such as Tang's method[12], which also generated comparable high-quality data.

To suppress the ligation of 5′-end primer fragments (after fragmentation) to the deep-sequencing library[12], we modified the amplification step by adding amine (NH_2) modification to the 5′-end bases of amplification primers on the C_6 linker. After amplification, primers and other potential nonspecific amplification by-products should be removed by gel purification or purification by beads. Using beads for purification led to less contamination and higher recovery efficiency, and it is recommended for batch operations. Although a high ratio of beads to PCR product increases the recovery efficiency of the short cDNA purification[39], we found that a high ratio of beads to DNA will

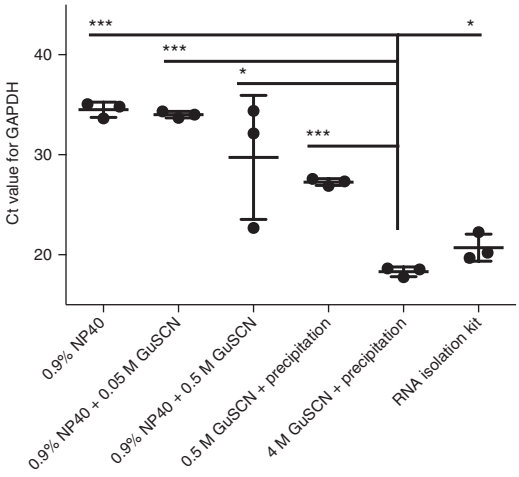

Figure 5 | Comparison of RNA quality of samples prepared under different lysis conditions. LCM samples with ~20 cells were lysed and precipitated with 0.9% NP40, 0.9% NP40 + 0.05 M GuSCN, 0.9% NP40 + 0.5 M GuSCN, 0.5 M or 4 M GuSCN, and then subjected to single-cell PCR analysis. Sample prepared using the Arcturus Picopure RNA Isolation Kit was included for comparison. 4 M GuSCN lysis with precipitation produced the best recovery (lowest GAPDH Ct value; $*P < 0.05$; $***P < 0.001$, three independent experiments were performed).

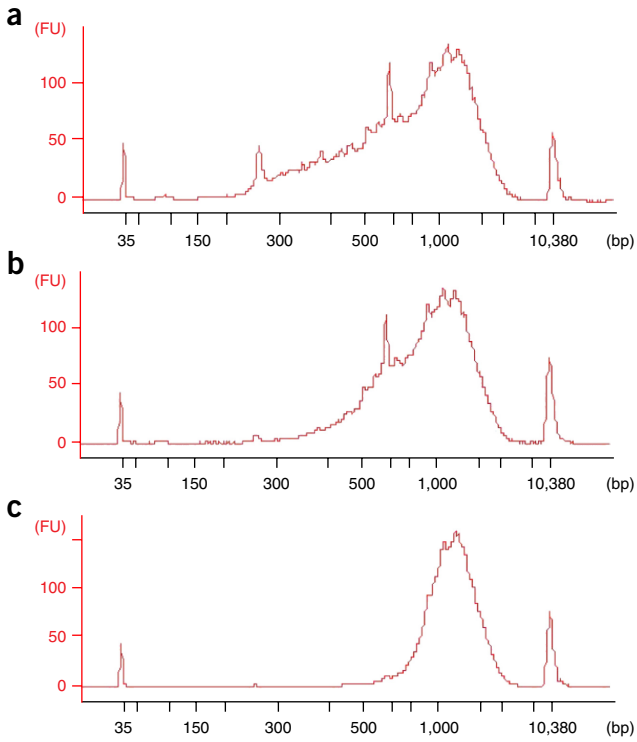

Figure 6 | Effect of different bead/DNA ratios on cDNA purification. (**a**–**c**) A bead/PCR ratio of 1:1 (**a**), 0.8:1 (**b**) or 0.6:1 (**c**) was used to purify PCR products. Primer dimers and short by-products could not be removed with a 1:1 ratio, whereas cDNA with a size of 500–700 bp was lost with a 0.6:1 ratio. The ratio of 0.8:1 produced a higher cDNA yield. FU, fluorescence units.

result in small fragments (shorter than 500 bp) being isolated (**Fig. 6a**). By contrast, the use of less beads will cause the loss of short fragments (**Fig. 6c**). The primer dimers and unspecific by-products can be efficiently eliminated using a 0.8 ratio of beads/PCR (**Fig. 6b**).

Data analysis for sequencing data. The quality of sequencing data—such as per-base sequence quality, mapping ratio, saturation and so on—should be evaluated first, before mapping all raw reads to the mouse genome (e.g., UCSC genome release mm10, https://genome.ucsc.edu/cgi-bin/hgGateway) and quantifying the expression level for each gene. To obtain stable domain information, unexpressed genes and genes with very low variance across all samples (expression levels are logarithmically transformed) were removed. Clustering analysis is performed to identify sample domains. Interdomain differentially expressed genes (DEGs) are then identified by pairwise comparison of these domains. The final domains could be determined by DEGs. Finally, a small set of key genes (the zip-code genes) that reflect spatial transcriptome information very similar to that of the DEGs, are identified and used for mapping cell populations or single cells to their home base.

Strengths and limitations of the protocol

Gene expression is regulated temporally and spatially. In previous studies, gene profiling was performed on thousands of cells in a sample or a collection of single cells with unknown spatial information. Although the LCM methods have been developed to harvest cells of interest, samples of thousands of cells must be pooled to provide enough starting material for RNA sequencing[26]. The Geo-seq protocol profoundly advances the analysis at a resolution of as few as ten cells, using a combination of established techniques that are modified for the specific purpose of elucidating a spatial transcriptome. It is a robust and cost-effective protocol that can be adapted for LCM capture of fluorescent samples if the apparatus is equipped with the appropriate fluorescence capacity to identify cells of interest in a defined location in the specimen.

Some limitations remain:

- The method of library preparation amplifies only mRNA with a poly(A) tail, an inherent limitation of the Smart2-seq method.
- Geo-seq cannot attain single-cell resolution with the current LCM technology because during sample preparation (cryosectioning and LCM) the quality of RNA can be compromised and many harvested cells do not remain intact after laser microdissection.
- Compared with methods of computational reconstruction[40–42], Geo-seq can be laborious, as it requires building a high-resolution transcriptome atlas based on positional capture of cell samples.

Applications of the method

The Geo-seq protocol is amenable to 3D profiling of gene expression for samples with limited availability for studying the relationship of regionalized gene expression and specific cell fate. Geo-seq is the ideal method for studying gene expression profiles with spatial variances in the activity of signaling pathways and the gene regulatory network. It is also amenable to studying the gene expression profile of rare cells such as adult stem cells and tumor-initiating cells in their respective niche. The Geo-seq

protocol can be applied to study the transcriptome of rare cells and their neighboring niche tissues, which may provide an entry point for understanding of the molecular mechanisms in cell lineage specification and differentiation, as well as cell–niche interactions in development and carcinogenesis.

Alternative methods

A similar approach, Tomo-seq, has been devised for spatial gene profiling[43]. The technique is based on the computational tomographic reconstruction of the RNA-seq data obtained from tissues in an orthogonal series of sections in multiple putatively identical biological samples. However, the data generated from different biological samples may introduce inherent variations that cannot be compensated for by computational meta-analysis. By contrast, Geo-seq generates 3D gene expression profiles from nonoverlapping domains in a single embryo or tissue, which minimizes potential artifacts, as well as nonreproducibility of sampling and the noise associated with computational reconstruction. A previous study by Zechel *et al.* using LCM and RNA-seq on mouse brain slices[26] revealed spatial resolution in a planar 2D context but not in 3D, as can be achieved by Geo-seq. In addition, transcripts of up to 2,236 genes per sample (of ~100 cells) were identified, in contrast to Geo-seq, which permits transcripts of >8,000 genes to be identified in samples of ~20 cells. The lower performance of Zechel's protocol could be because of lower RNA recovery efficiency, as the authors lyse LCM samples directly in a small volume of mild dissociation solution. Two computational methods have been developed for the spatial reconstruction of single-cell gene expression data[40,41], both of which rely on known spatial expression data from reference genes. By contrast, the Geo-seq protocol enables the construction of spatial expression map of genes *de novo* with high levels of reproducibility and fidelity[28].

MATERIALS

REAGENTS

- Mouse embryos (obtained from pregnant C57BL/6E mice (The Jackson Laboratory)) or other fresh tissues of interest, such as fresh brain or tumor tissues **! CAUTION** Experiments using rodents must conform to national and institutional regulations. Our experiments conformed to Shanghai Institute of Biochemistry and Cell Biology guidelines.
- RNase-Zap (Ambion, cat. no. AM9780)
- Tissue freezing medium (OCT; Leica Microsystems, cat. no. 020108926)
- Cresyl violet acetate (Sigma-Aldrich, cat. no. C5042)
- Guanidine isothiocyanate (GuSCN) solution (4 M GuSCN, 50 mM Tris–HCl (pH 7.5), 25 mM EDTA; Invitrogen, cat. no. 15577-018)
- Ethanol (SinoPharm Shanghai)
- PBS (Thermo Fisher Scientific, cat. no. 10010023)
- Glycogen (20 mg/1 ml; Roche, cat. no.10901393001)
- Sodium acetate (3 M, pH 5.5; Ambion, cat. no. AM9740)
- dNTP mix (2.5 mM each; Takara, cat. no. 4030)
- Nuclease-free water (Ambion, cat. no. AM9930)
- Protector RNase inhibitor (Roche, cat. no. 03335399001)
- DTT (Invitrogen, cat. no. 18064-014)
- SuperScript II reverse transcriptase (Invitrogen, cat. no. 18064-014)
- Betaine solution (5 M, PCR reagent; Sigma-Aldrich, cat. no. B0300-1VL)
- Magnesium chloride ($MgCl_2$; 1.00 M±0.01 M; Sigma-Aldrich, cat. no. M1028-100ML)
- KAPA HiFi HotStart ReadyMix (2×; KAPA Biosystems, cat. no. KK2601)
- Agencourt AMPure XP beads (Beckman Coulter, cat. no. A 63881)
- 3′ CDS, LNA-TSO and A-IS primers were ordered from Sangon Biotech (Shanghai, China)
- Nextera XT DNA Sample Preparation Kit, 96 samples (Illumina, cat. no. FC-131-1096)
- Nextera XT 24-Index Kit, 96 samples (Illumina, cat. no. FC-131-1001)
- TruSeq Dual-index Sequencing Primer Kit for single-read runs (Illumina, cat. no. FC-121-1003) or paired-end runs (Illumina, cat. no. PE-121-1003)

EQUIPMENT

- Cryostat (Leica Mycrosystems, cat. no. CM1950)
- CellCut laser microdissection system (CellCut System; MMI)
- PEN Membrane slide (MMI, cat. no. 50102)
- IsolationCap (0.2 ml; MMI, cat. no. 50206)
- Microcentrifuge tube (Axygen, cat. no. MCT-150-NC)
- Thermal cycler (Applied Biosystems, cat. no. 9700)
- Centrifuge, scan speed: 1730R (Labocene)
- PCR magnet (Applied Biosystems, cat. no. 49-2025)
- Thin-walled PCR tubes with caps (Axygen, cat. no. PCR-02-L-C)
- Filter tips: 10-, 20-, 200- and 1,000-µl (Axygen, cat. nos. TF-300-R-S, TF-20-R-S, TF-200-R-S, TF-1000-R-S)
- Qubit assay tubes (Invitrogen, cat. no. Q32856)
- Qubit dsDNA High-Sensitivity (HS) Kit (Invitrogen, cat. no. Q32851)
- Qubit 2.0 Fluorometer (Invitrogen, cat. no. Q32866)
- Agilent 2100 Bioanalyzer (Agilent Technologies, cat. no. G2938C)
- Agilent High-Sensitivity DNA Kit (Agilent Technologies, cat. no. 5067-4626)
- Whatman no. 1 filter paper (Sigma-Aldrich, cat. no. 1001110)

REAGENT SETUP

3′ CDS primer (5′-AAGCAGTGGTATCAACGCAGAGTACT$_{30}$VN-3′) At the 3′ end, 'N' is any base and 'V' is A, C or G. Dissolve the oligonucleotide in dH_2O to a final concentration of 10 µM. Store this oligo at −20 °C for up to 6 months.

LNA-TSO primer (5′-AAGCAGTGGTATCAACGCAGAGTACATrGrG+G-3′) At the 3′ end, there are two riboguanosines (rGs) and one LNA-modified guanosine (+G). Dissolve LNA-TSO in dH_2O to a final concentration of 100 µM. Split into small aliquots and store them at −80 °C for up to 6 months, avoiding repeated freeze–thaw cycles.

A-IS PCR primer (5′-AAGCAGTGGTATCAACGCAGAGT-3′) Amine (NH_2) modification was added to the 5′ end with a C_6 linker during synthesis. Dissolve the oligonucleotide in dH_2O to a final concentration of 10 µM. This primer can be stored at −20 °C for up to 6 months.

Cresyl violet staining solution Dissolve cresyl violet powder to 1% (wt/vol) with 70% (vol/vol) ethanol. Filter the staining solution with Whatman no. 1 filter paper and store it at room temperature (18–25 °C).

PROCEDURE

Tissue collection and embedding ● TIMING 45 min

▲ **CRITICAL** All the tools and reagents should be RNase-free, and all the procedures should be done as quickly as possible.

▲ **CRITICAL** We describe carrying out the analysis on mouse embryos; alternative source tissues can be used. If other freshly collected tissues are available, you can start from Step 3, omitting Steps 1 and 2.

1| On the day of interest, kill the pregnant mouse with cervical dislocation according to animal ethics guidelines. Make an incision into the abdominal cavity.

2| Remove the uterine horns and place them in cold RNase-free PBS. Gently cut the muscle along the uterus with forceps to pinch off the individual decidua inside, each of which contains an embryo.
▲ **CRITICAL STEP** Conservation of supporting tissues such as decidua for mouse embryos is important to retaining good morphology during tissue collection, embedding and cryosectioning. Open some of the decidua and collect embryos for verification of the proper stage under the dissection microscope.

3| Gently transfer the mouse decidua into a cryomold and remove the PBS. Add precooled OCT compound. Gently move the tissues down to near the bottom of the cryomold. At the same time, make sure that the embryo is standing vertically in the OCT compound in the cryomold.

4| Immediately freeze the embryo in liquid nitrogen or dry ice. Make sure that the mold is in a stable horizontal position.

5| When the OCT compound is completely frozen, transfer the tissue to –80 °C.
■ **PAUSE POINT** The tissue can be stored at –80 °C for several weeks.

Cryosectioning ● TIMING 30 min
! CAUTION Take care to avoid injury by the cryostat blade.
6| Clean the cryostat and insert a new sterile blade. Set the temperature on the cryostat to –20 °C and the cutting thickness to 15 µm (this can be adjusted depending on the size of the tissue and the resolution of the cutting).

7| Remove the frozen block of OCT compound from the cryomold, trim it as necessary and affix it to a metal stage at the OCT for cryosectioning.

8| Section the entire tissue of interest onto LCM PEN membrane slides. UV light treatment of the slide can sterilize the sample and increase adherence. Do not expose the slide to UV light for longer than 30 min, as there is a risk of damaging the membrane.
! CAUTION UV light is harmful to human skin and eyes. Avoid direct exposure to UV light.

Staining with cresyl violet ● TIMING 5 min
9| Place the membrane slides with cryosections in 100% (vol/vol) ethanol for 30 s.

10| Place the slides into 95% (vol/vol) and 70% (vol/vol) ethanol solution for 30 s each.

11| Stain with 1% (wt/vol) cresyl violet in 70% (vol/vol) ethanol for 1 min.

12| Dehydrate the slides in 70, 90 and 100% (vol/vol) ethanol for 30 s each.

13| Place the slides at room temperature for 1–2 min until they are dry. Adequate dehydration is critical to minimizing RNase activity and the adhesive force between the slide and the tissue.
? TROUBLESHOOTING

Laser capture microdissection ● TIMING 20 min–2 h
14| Make a sandwich by putting a cover-glass slide under the stained membrane slide.

15| Place the sandwich slide onto the objective stage.

16| Scan the slide with a 4× objective to get an overview of the whole slide.

17| Choose an appropriate objective, and adjust laser energy, focus and cutting speed.
▲ **CRITICAL STEP** Laser energy, focus and cutting speed are critical to laser microdissection. For example, a laser energy setting that is too weak does not cut the tissue, whereas one that is too strong destroys surrounding RNA.

18| Cut target cells, and collect them with IsolationCaps.
! CAUTION There is invisible laser radiation during the cutting process. Do not stare into the beam or view it with optical instruments.
? TROUBLESHOOTING

19| Check the LCM samples collected on the IsolationCaps under a microscope.

Lysis and RNA extraction ● TIMING 2 h

20| Add 50 µl of 4 M GuSCN solution to the tube bottoms of the IsolationCaps.
! CAUTION GuSCN solution is corrosive. Avoid contact with skin and eyes.

21| After gently closing the cap of the collecting tube, invert the tube and make sure that all the lysis buffer is sitting on top of the cap.

22| Incubate the tube at 42 °C for 15 min upside-down.

23| Centrifuge the samples for 30 s at 7,000*g* at 4°C. Transfer the lysis buffer to a 1.5-ml microcentrifuge tube, and put it on ice immediately.

24| Prepare a precipitating buffer (771 µl per sample) by combining and mixing the following components:

Component	Volume (µl)	Final concentration
Nuclease-free water	150	
Ethanol	600	78%
Sodium acetate (1.5 M pH 6.5)	20	0.04 M
Glycogen (20 mg/ml)	1	20 µg
Total volume	771	

25| Add 771 µl of the mix to each sample tube, and mix thoroughly. Then, incubate at –80 °C for at least 30 min.
■ PAUSE POINT The mixture can be kept at –80 °C for as long as one month.

26| Centrifuge the samples for 30 min at 12,000*g* at 4 °C.

27| Discard the supernatant and wash the pellet with 75% (vol/vol) ethanol solution and centrifuge for another 10 min at 12,000*g* at 4 °C.

28| Discard the supernatant, and remove remaining fluid with tips. Air-dry the RNA pellet briefly at room temperature.
▲ CRITICAL STEP Make sure that once the pellet becomes invisible, you move on to the next step immediately. It is good to mark the location of the pellet before this step, because the volume of the dissolution buffer in the next step is very small.

RNA dissolution and denaturation ● TIMING 10 min

29| Prepare 4.56 µl of dissolution buffer for each sample by combining and mixing the following components:

Component	Volume (µl)	Final concentration
Nuclease-free water	2.51	
3′ CDS primer (10 µM)	1	1 µM
dNTP (10 mM)	1	1 mM
RNase inhibitor (40 U/µl)	0.05	2 U
Total volume	4.56	

30| Add 4.56 µl of precooled dissolution buffer to the above pellet.

31| Dissolve the pellet by gently pipetting up and down a few times without forming bubbles. Then transfer the RNA to a 0.2-ml thin-walled PCR tube, and put it on ice.
▲ CRITICAL STEP Ensure that no bubbles form during dissolution.

32| Incubate the samples at 72 °C for 3 min for denaturation and immediately put them back on ice.

33| Centrifuge the samples for 30 s at 7,000*g* at 4 °C.

Reverse transcription ● TIMING 3.5 h

34| Prepare the reverse transcription (RT) mix as follows:

Component	Volume (µl)	Final concentration
SuperScript II reverse transcriptase (200 U/µl)	0.5	100 U
RNAse inhibitor (40 U/µl)	0.25	10 U
SuperScript II first-strand buffer (5×)	2	1×
DTT (100 mM)	0.5	5 mM
Betaine (5 M)	2	1 M
$MgCl_2$ (1 M)	0.09	9 mM
LNA-TSO (100 µM)	0.1	1 µM
Total volume	5.44	

35| Add 5.44 µl of the RT mix to the samples from Step 33 to obtain a final reaction volume of 10 µl.

36| Centrifuge the samples for 30 s at 7,000*g* at 4 °C. Carry out the following PCR program to reverse-transcribe the RNA.

Number of cycles	42 °C	50 °C	42 °C	70 °C	4 °C
1–10	90 min	2 min	2 min		
11				15 min	
12					Hold

▲ **CRITICAL STEP** The reaction temperature for SuperScript II reverse transcriptase should be maintained at 42 °C. The following ten cycles are needed to open some RNA secondary structures (such as hairpins or loops).

37| Centrifuge the samples for 30 s at 7,000*g* at 4 °C.

cDNA preamplification ● TIMING 3.5 h

38| Prepare 15 µl of PCR mix for each sample as follows:

Component	Volume (µl)	Final concentration
KAPA HiFi HotStart ReadyMix (2×)	12.5	1 ×
A-IS PCR primers (10 µM)	1	0.1 µM
Nuclease-free water	1.5	
Total volume	15	

▲ **CRITICAL STEP** HotStart PCR polymerase is strongly recommended to reduce nonspecific products.

39| Add 15 µl of the RT mix to the samples from Step 37 to obtain a final reaction volume of 25 µl.

40| Carry out the following PCR program:

Number of cycles	98 °C	67 °C	72 °C	4 °C
1	3 min			
2–20	20s	15s	6 min	
21			5 min	
22				Hold

▲ **CRITICAL STEP** The number of PCR cycles depends on the input amount of RNA. Generally, 16–19 cycles are suitable for most applications.

Quality check of PCR product ● TIMING 3 h

41| Take 2 µl from each sample and dilute 20-fold with nuclease-free water.

42| To test the quality of single-cell-based PCR, use 2 µl of diluted PCR product as a template to perform a 20-µl real-time qPCR reaction to check the expression of housekeeping genes such as *GAPDH*, *Actb* and *Hprt*. The Ct value of a good sample is usually <20.

? TROUBLESHOOTING

■ **PAUSE POINT** The remaining undiluted PCR product can be saved at –80 °C for several months.

Bead purification ● TIMING 45 min

▲ **CRITICAL** Make sure that no beads are pipetted out throughout the whole purification procedure.

43| Equilibrate AMPure XP beads to room temperature, and then vortex thoroughly for several seconds.

44| Add 17.6 µl of AMPure XP beads (0.8:1 ratio) to the PCR product (leaving ~22 µl). Mix thoroughly by pipetting up and down ten times and then incubate at room temperature for 8 min to let the cDNA bind to the beads.

45| Place the mixture on ae magnetic stand for at least 5 min, until the supernatant is completely clear.

46| While the tube is sitting on the magnetic stand, remove the supernatant carefully without pipetting out any beads.

47| Wash the beads with freshly made 80% (vol/vol) ethanol. Make sure that the beads remain on the inner surface of the tube without disturbing them during the process.

48| Repeat Step 47 one more time.

49| Briefly spin down for 10 s at 1,000*g* at room temperature to collect the liquid at the bottom of the tube.

50| Place the tube on the magnetic stand for 30 s, and then remove any trace of ethanol with a 10-µl tip.

51| Place the plate at room temperature for ~3–5 min, until the beads appear dried.

52| Add 16 µl of 0.1× TE to cover the beads, and resuspend the beads by pipetting up and down ten times.

53| Incubate the mixture for 2 min at room temperature off the magnet to elute DNA from the beads.

54| Put the tube back on the magnetic stand and leave it until the solution is completely clear.

55| Transfer the supernatant containing purified cDNA to a new nuclease-free tube.

■ **PAUSE POINT** The cDNA can be stored at –80 °C for 6 months.

Quality check of purified cDNA library ● TIMING 1 h

56| Quantify purified cDNA on a Qubit Fluorometer with a dsDNA HS assay kit.

57| Check the cDNA size distribution on an Agilent high-sensitivity DNA chip. The cDNA library should be free of short (<400 bp) fragments and should show a peak ~1.5–2 kb.
? TROUBLESHOOTING

cDNA digestion ● TIMING 20 min
58| Digest up to 1 ng of purified cDNA library with transposase in an Illumina Nextera XT DNA Sample Preparation Kit at 55 °C for 5 min. Make up the digestion mixture as follows and put on ice immediately after digestion:

Component	Volume (μl)
cDNA	1–5
Tagment DNA Buffer (TD)	10
Amplicon Tagment Mix (ATM)	5
Nuclease-free water	0–4
Total volume	20

▲ **CRITICAL STEP** The total amount of cDNA should not exceed 1 ng when using the Illumina Nextera XT DNA Sample Preparation Kit.

59| Add 5 μl of Neutralize Tagment Buffer (provided in the Nextera Library Preparation Kit) for 5 min at room temperature to stop the reaction.

PCR enrichment ● TIMING 1 h
60| Add the following components from the Illumina Nextera XT DNA Sample Preparation Kit directly to the above reaction mixture and mix well:

Component	Volume (μl)
cDNA	25
Index 1 (N7XX) primers	5
Index 2 (N5XX) primers	5
Nextera PCR Master Mix (NPM)	15
Total volume	50

61| Carry out the following PCR program:

Number of cycles	72 °C	95°C	55 °C	72 °C	4 °C
1	3 min	30s			
2–13		10s	30s	30s	
14				5 min	
15					Hold

Bead purification of amplified library ● TIMING 2 h
62| Purify adaptor-ligated DNA from Step 61 (with 50 μl of AMPure XP beads, ratio 1:1) as described in Steps 43–55, and elute with 50 μl of 0.1× TE.

63| Check the size distribution on an Agilent Bioanalyzer high-sensitivity chip.

cDNA sequencing ● TIMING ~2 d
64| Sequence the cDNA on an Illumina HiSeq platform at a depth of 20 million reads per library.

Preliminary processing of sequencing data ● TIMING ~3 d; time varies based on samples to be analyzed

65| After performing RNA sequencing for all samples, evaluate the quality of the raw reads by FASTQC. To do this, first map the reads for each sample to the mouse genome (mm10) using TopHat[44].

66| Count the number of mapped reads for each sample and then calculate the mapping ratio (remove samples with low mapping ratios).

67| Generate a saturation curve for each sample to evaluate whether all expressed genes are detected (remove or add sequencing for failed samples).

68| Quantify gene expression levels (fragments per kilobase of transcript per million mapped reads (FPKM)) based on mapped reads by using Cufflinks[45] or another acceptable evaluation method.

69| Identify expressed genes with the criterion FPKM>1.0 (or another expression evaluation method) in at least two samples across all samples (parameters must be modified depending on specific contexts).

Gene clustering and zip-code gene identification ● TIMING ~2 d

70| Transform the original FPKM values into logarithmic space by using the $\log_{10}$(FPKM+1) or another acceptable logarithmic space.

71| Calculate and plot density distributions for all samples based on the expressed genes (remove samples with inconsistent distribution).

72| Filter genes with a variance in transcript levels ($\log_{10}$(FPKM + 1)) across all samples <0.05, and use the remaining genes (defined as the selected gene set) for the following analysis. (Parameters must be modified depending on specific contexts.)

73| Perform unsupervised hierarchical clustering with a correlation distance metric to classify all samples into different domains (a distinctly separated dendrogram) based on *z*-score-normalized $\log_2$(FPKM) of the selected gene set.

74| Identify inter-domain DEGs by performing pairwise comparison among different domains (in Step 72), and genes with a *t* test[46] *P* value <0.01 and mean fold change >2.0 or <0.5 are selected as DEGs. (Parameters must be modified depending on specific contexts.)

75| *z*-score-normalize $\log_2$(FPKM) of DEGs across all samples, and then perform BIC-SKmeans[47] clustering for DEGs to identify the final gene groups and perform hierarchical clustering with a correlation distance metric to determine the final sample groups/domains.

76| Identify the zip-code genes by selecting the genes with the highest or lowest principal component analysis (PCA) loadings (calculated with FactoMineR in R) in the first several PCs. (Parameters need to be modified depending on specific contexts.)
▲ CRITICAL STEP The clustering pattern for all samples based on zip-code genes must be very similar to the result based on DEGs, and thus almost all the spatial transcriptome information will be kept. Try to obtain suitable parameters in this step to optimize the zip-code gene list.

Spatial information visualization and integration ● TIMING ~3 d; this does not include time for design process and zip-code mapping

77| Design a 2D plot to visualize the spatial structure of the research object based on its morphology (we used corn plots in our paper[28]). The expression pattern for each gene can be clearly displayed in the designed plot. Corn plot visualization and zip-code mapping can be performed through the iTranscriptome portal at http://www.itranscriptome.org.

78| Perform zip-code mapping by calculating the Spearman rank correlation coefficients (RCCs) between all samples and the user's query transcriptome data (single cells or cell population) based on the expression of zip-code genes.

79| Visualize the RCC values (in Step 77) in the designed plot for each query sample, and a higher RCC value indicates a strong probability of a matching position.

80| Apply a smoothing procedure to fit the query sample's location as a diffused domain. In this step, each RCC value should be mapped on the designed plot by calculating the average value of this RCC and the RCCs of samples from adjacent regions in the same spatial domain. The final diffused domain encompasses the region with the top smoothed RCC values.

? TROUBLESHOOTING

Troubleshooting advice can be found in **Table 1**.

TABLE 1 | Troubleshooting table.

Step	Problem	Possible reason	Solution
13	Structure of the cryosection is destroyed after staining	OCT compound on the section was not dry before staining	Make sure that the OCT compound on the section is dry before staining
18	Section could not be cut by laser	LCM system parameters were not correct	Adjust LCM parameters (laser energy, focus and cut speed) to match the individual needs of each application, sample or objective before cutting target cells
		Laser energy was attenuated	Restart laser or software, or change to a new laser exciter
42	The expression level of housekeeping genes is very low	The RNA was degraded before reverse transcription	Make sure that all the reagents and tools are RNase-free. All the processes should be performed as quickly as possible. Place the samples on ice if possible
		LCM sample was not collected by IsolationCap	Check whether LCM samples are on IsolationCap after capture
		RNA pellet was not dry before adding dissolution buffer	Make sure that the RNA pellet is dry and that there is no ethanol or water remaining
		Loss of activity of some enzymes or reagents	Change to new enzymes/reagents or a new lot
		Riboguanosines at the 3′ end of the TSO primer degrade	Order new LNA-TSO primer. Prepare aliquots and store at –80 °C, avoiding repeated freeze–thaw cycles
57	Primer dimers and short fragments (<300 bp) remain after bead purification	Too many beads were added	Reduce bead/PCR product ratio
	cDNAs longer than 500 bp were lost after bead purification	Too few beads present	Increase bead/PCR product ratio
	cDNA library peak is lower than 1.5 kb	The RNA degraded	Make sure that all the reagents and tools are RNase-free. All the processes should be performed as quickly as possible. Place the samples on ice if possible

● TIMING

Day 1

Steps 1–5, tissue collection and embedding: 45 min

Steps 6–8, cryosectioning: 30 min

Steps 9–13, staining: 5 min

Steps 14–19, laser capture microdissection: 20 min—2 h

Steps 20–28, lysis and RNA extraction: 2 h

Day 2

Steps 29–33, RNA dissolution and denaturation: 10 min

Steps 34–37, reverse transcription: 3.5 h

Steps 38–40, cDNA preamplification: 3.5 h

Steps 41 and 42, quality check of PCR product: 3 h

Day 3

Steps 43–55, bead purification: 45 min

Steps 56 and 57, quality check of purified cDNA library: 1 h

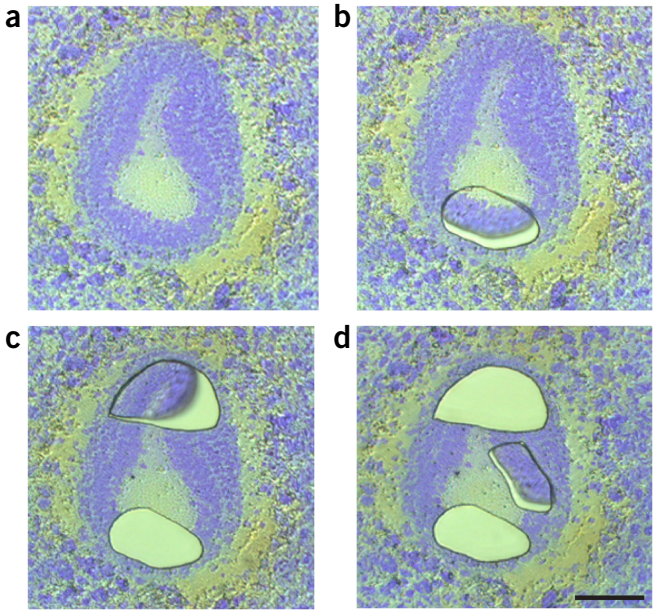

Figure 7 | Laser microdissection of cryosections of gastrula-stage mouse embryo (corresponding to Step 19). (**a**) Cryosection of gastrula-stage mouse embryo before laser microdissection. (**b**–**d**) Samples of ~20 cells each in (**b**) anterior, (**c**) posterior and (**d**) left lateral epiblast were captured by laser microdissection. Scale bar, 50 µm.

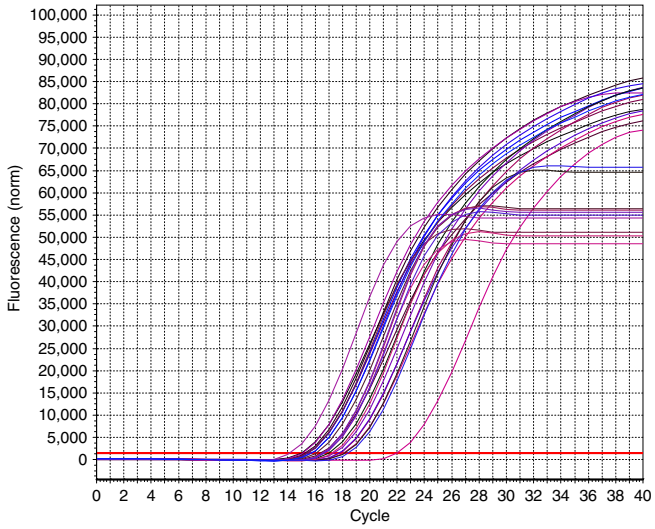

Figure 8 | Real-time PCR amplification plot of GAPDH in representative LCM samples (corresponding to Step 42). The GADPH expression of 24 LCM samples, with typical Ct values at 16–18. norm, normalized.

Steps 58 and 59, cDNA digestion: 20 min
Steps 60 and 61, PCR enrichment of adaptor-ligated cDNA: 1h
Steps 62 and 63, bead purification of the amplified library: 2 h

Day 4–5

Step 64, cDNA sequencing: ~2 d

Days 6–14

Step 65–80, sequencing data analysis: ~1 week

ANTICIPATED RESULTS

Step 19

Figure 7 presents an example of a gastrulating mouse embryo cryosection before (**Fig. 7a**) and after LCM (**Fig. 7b–d**). The morphology of the samples was maintained and different samples were clearly cut without burning surrounding cells.

Step 42

Unsuccessful tissue or sample processing will result in a poor cDNA yield. The typical Ct value for the housekeeping gene *GADPH* for conventional cell types is ~16–18 if 10–20 cells are captured with LCM (**Fig. 8**). The amount of cDNA will not be enough for sequencing library preparation if the Ct value of *GAPDH* is higher than 25.

Step 56

Usually, LCM samples of ~20 cells yield tens or even more than one hundred nanograms of cDNA, which is enough for low-input cDNA sequencing. The quantities of cDNA that we obtained after purification for regular 20-cell LCM samples are listed in **Table 2**.

Step 57

Representative cDNA library size distribution is shown in **Figure 9**. A good cDNA library should be free of short fragments (<500 bp) and have a peak at ~1.5–2 kb.

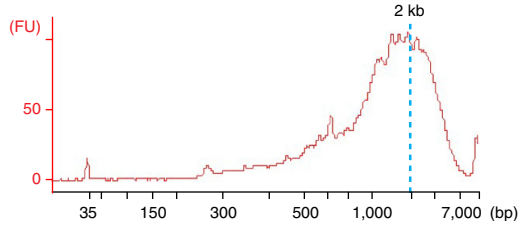

Figure 9 | Bioanalyzer electropherogram of cDNA libraries (corresponding to Step 57). Size distribution of cDNA library assessed in an Agilent 2100 bioanalyzer is shown. The preparation was free of primer dimers and short fragments (<500 bp), with the peak size at 1.5–2 kb (more than three independent experiments were performed).

TABLE 2 | Quantity of cDNA library after purification.

Sample no.	Ct value for *GAPDH*	Conc. (ng/μl)	Total amount (ng)
1	14.94	10.2	163.2
2	15.35	9.82	157.12
3	16.50	4.04	64.64
4	15.43	9.06	144.96
5	17.85	3	48
6	18.13	3	48
7	22.00	0.542	8.672
8	15.05	7.76	124.16
9	17.46	3.28	52.48
10	17.79	3.82	61.12
11	15.80	7.4	118.4
12	15.58	7.48	119.68
13	16.99	5.24	83.84
14	18.22	2.86	45.76
15	16.02	5.08	81.28
16	15.53	7.4	118.4
17	16.64	4.38	70.08
18	17.33	3.92	62.72
19	16.77	4.48	71.68
20	14.21	13	208
21	16.63	4.74	75.84
22	16.75	5.04	80.64
23	18.50	1.6	25.6
24	15.77	4.84	77.44

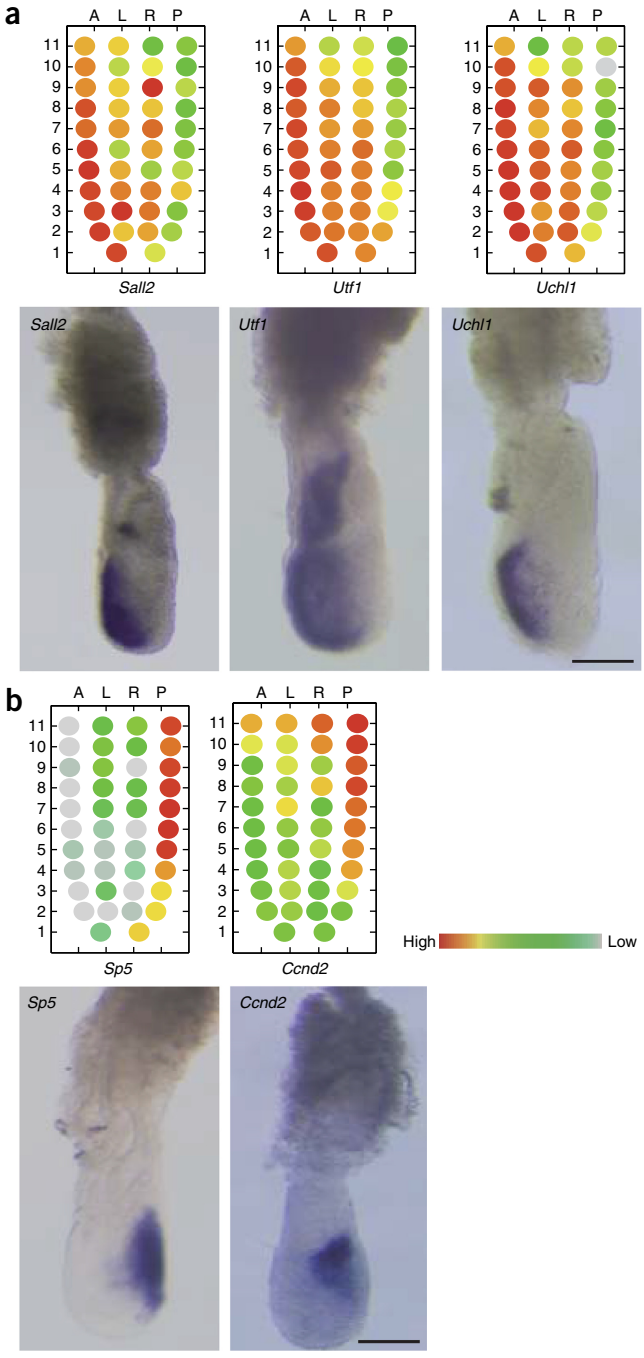

Figure 10 | Examples of Geo-seq results showing high spatial resolution of gene expression pattern (displayed as corn plots) in the mid-gastrula-stage mouse embryo (corresponding to Step 77). (**a**) Upper panel: corn plot of the distribution of transcripts of *Sall2*, *Utf1* and *Uch1* in the anterior epiblast; lower panel: corresponding WISH images. (**b**) Upper panel: corn plot of the distribution of transcripts *Sp5* and *Ccnd2* in the posterior epiblast; lower panel: corresponding WISH images. Scale bars, 200 μm. Image adapted with permission from ref. 28, Elsevier/Cell Press.

Steps 65–69

For each of 42 LCM samples captured from an embryonic day (E)7.0 mouse embryo, we sequenced 20 million reads, and all the mapping ratios were >80%. The readily detectable unique genes ranged from 8,000 to 10,000 for each LCM sample. We also performed genome-wide profiling on three individual embryo replicates, and the similarity between embryos was very high, suggesting that this method is robust and highly reproducible[28].

Step 77

Examples of genes with spatially restricted expression are shown in **Figure 10**. The newly identified anterior-specific genes *Sall2*, *Utf1* and *Uchl1* were exclusively expressed in the anterior epiblast, whereas *Sp5* and *Ccnd2* were confined to the posterior region. The 2D corn plot for these genes showed a high correlation with whole-mount *in situ* hybridization (WISH) images (WISH procedure in **Supplementary Methods**).

Note: Any Supplementary Information and Source Data files are available in the online version of the paper.

ACKNOWLEDGMENTS We are grateful to Q. Zhou (Institute of Zoology, Chinese Academy of Sciences) for helpful suggestions, and to Y. Qian of the Jing laboratory for technical support. The sequencing was performed on an Illumina HiSeq2500 system by BerryGenomics (Beijing, China). This work was supported in part by the 'Strategic Priority Research Program' of the Chinese Academy of Sciences (XDA01010201 to N.J., XDB19020301 and XDA01010303 to J.-D.J.H.), the National Key Basic Research and Development Program of China (2014CB964804 and 2015CB964500 to N.J., and 2015CB964803 and 2016YFE0108700 to J.-D.J.H.) and the National Natural Science Foundation of China (31430058, 31571513, 31630043, 91519314 to N.J., and 91329302, 31210103916, 91519330 to J.-D.J.H.).

AUTHOR CONTRIBUTIONS N.J. supervised the project. N.J. and G.P. designed the experiment. J.C. and G.P. performed the laser microdissection and RNA-seq. J.C. and S.S. wrote the manuscript. G.P., P.P.L.T., J.-D.J.H. and N.J. edited the manuscript.

COMPETING INTERESTS STATEMENT The authors declare no competing financial interests.

1. Dalerba, P. *et al.* Single-cell dissection of transcriptional heterogeneity in human colon tumors. *Nat. Biotechnol.* **29**, 1120–1127 (2011).
2. Cann, G.M. *et al.* mRNA-Seq of single prostate cancer circulating tumor cells reveals recapitulation of gene expression and pathways found in prostate cancer. *PLoS One* **7**, e49144 (2012).
3. Shalek, A.K. *et al.* Single-cell transcriptomics reveals bimodality in expression and splicing in immune cells. *Nature* **498**, 236–240 (2013).
4. Buganim, Y. *et al.* Single-cell expression analyses during cellular reprogramming reveal an early stochastic and a late hierarchic phase. *Cell* **150**, 1209–1222 (2012).
5. van Wolfswinkel, J.C., Wagner, D.E. & Reddien, P.W. Single-cell analysis reveals functionally distinct classes within the planarian stem cell compartment. *Cell Stem Cell* **15**, 326–339 (2014).
6. Guo, G. *et al.* Resolution of cell fate decisions revealed by single-cell gene expression analysis from zygote to blastocyst. *Dev. Cell* **18**, 675–685 (2010).
7. Yan, L. *et al.* Single-cell RNA-Seq profiling of human preimplantation embryos and embryonic stem cells. *Nat. Struct. Mol. Biol.* **20**, 1131–1139 (2013).
8. Durruthy-Durruthy, R. *et al.* Reconstruction of the mouse otocyst and early neuroblast lineage at single-cell resolution. *Cell* **157**, 964–978 (2014).
9. Xue, Z. *et al.* Genetic programs in human and mouse early embryos revealed by single-cell RNA sequencing. *Nature* **500**, 593–597 (2013).
10. Hebenstreit, D. Methods, challenges and potentials of single cell RNA-seq. *Biology* **1**, 658–667 (2012).
11. Tang, F. *et al.* mRNA-Seq whole-transcriptome analysis of a single cell. *Nat. Methods* **6**, 377–382 (2009).
12. Tang, F. *et al.* RNA-Seq analysis to capture the transcriptome landscape of a single cell. *Nat. Protoc.* **5**, 516–535 (2010).
13. Hashimshony, T., Wagner, F., Sher, N. & Yanai, I. CEL-Seq: single-cell RNA-Seq by multiplexed linear amplification. *Cell Rep.* **2**, 666–673 (2012).
14. Islam, S. *et al.* Highly multiplexed and strand-specific single-cell RNA 5′ end sequencing. *Nat. Protoc.* **7**, 813–828 (2012).
15. Goetz, J.J. & Trimarchi, J.M. Transcriptome sequencing of single cells with Smart-Seq. *Nat. Biotechnol.* **30**, 763–765 (2012).
16. Picelli, S. *et al.* Full-length RNA-seq from single cells using Smart-seq2. *Nat. Protoc.* **9**, 171–181 (2014).
17. Picelli, S. *et al.* Smart-seq2 for sensitive full-length transcriptome profiling in single cells. *Nat. Methods* **10**, 1096–1098 (2013).
18. Wen, L. & Tang, F. Single-cell sequencing in stem cell biology. *Genome Biol.* **17**, 71 (2016).
19. Shapiro, E., Biezuner, T. & Linnarsson, S. Single-cell sequencing-based technologies will revolutionize whole-organism science. *Nat. Rev. Genet.* **14**, 618–630 (2013).
20. Liu, A. Laser capture microdissection in the tissue biorepository. *J. Biomol. Tech.* **21**, 120–125 (2010).
21. Datta, S. *et al.* Laser capture microdissection: big data from small samples. *Histol. Histopathol.* **30**, 1255–1269 (2015).
22. Canas, R.A., Canales, J., Gomez-Maldonado, J., Avila, C. & Canovas, F.M. Transcriptome analysis in maritime pine using laser capture microdissection and 454 pyrosequencing. *Tree Physiol.* **34**, 1278–1288 (2014).
23. Erickson, H.S. *et al.* Quantitative RT-PCR gene expression analysis of laser microdissected tissue samples. *Nat. Protoc.* **4**, 902–922 (2009).
24. Morrison, J.A., Bailey, C.M. & Kulesa, P.M. Gene profiling in the avian embryo using laser capture microdissection and RT-qPCR. *Cold Spring Harbor Protoc.* **2012**, 1249–1262 (2012).
25. Grover, P.K., Cummins, A.G., Price, T.J., Roberts-Thomson, I.C. & Hardingham, J.E. A simple, cost-effective and flexible method for processing of snap-frozen tissue to prepare large amounts of intact RNA using laser microdissection. *Biochimie* **94**, 2491–2497 (2012).
26. Zechel, S., Zajac, P., Lonnerberg, P., Ibanez, C.F. & Linnarsson, S. Topographical transcriptome mapping of the mouse medial ganglionic eminence by spatially resolved RNA-seq. *Genome Biol.* **15**, 486 (2014).
27. Bandyopadhyay, U., Fenton, W.A., Horwich, A.L. & Nagy, M. Production of RNA for transcriptomic analysis from mouse spinal cord motor neuron cell bodies by laser capture microdissection. *J. Vis. Exp.* **83**, e51168 (2014).
28. Peng, G. *et al.* Spatial transcriptome for the molecular annotation of lineage fates and cell identity in mid-gastrula mouse embryo. *Dev. Cell* **36**, 681–697 (2016).
29. Cox, M.L. *et al.* Assessment of fixatives, fixation, and tissue processing on morphology and RNA integrity. *Exp. Mol. Pathol.* **80**, 183–191 (2006).
30. Goldsworthy, S.M., Stockton, P.S., Trempus, C.S., Foley, J.F. & Maronpot, R.R. Effects of fixation on RNA extraction and amplification from laser capture microdissected tissue. *Mol. Carcinog.* **25**, 86–91 (1999).
31. Wang, W.Z., Oeschger, F.M., Lee, S. & Molnar, Z. High quality RNA from multiple brain regions simultaneously acquired by laser capture microdissection. *BMC Mol. Biol.* **10**, 69 (2009).
32. Parlato, R. *et al.* A preservation method that allows recovery of intact RNA from tissues dissected by laser capture microdissection. *Anal. Biochem.* **300**, 139–145 (2002).
33. Wang, H. *et al.* Histological staining methods preparatory to laser capture microdissection significantly affect the integrity of the cellular RNA. *BMC Genomics* **7**, 97 (2006).
34. Sonne, S.B. *et al.* Optimizing staining protocols for laser microdissection of specific cell types from the testis including carcinoma *in situ*. *PLoS One* **4**, e5536 (2009).
35. Clement-Ziza, M., Munnich, A., Lyonnet, S., Jaubert, F. & Besmond, C. Stabilization of RNA during laser capture microdissection by performing experiments under argon atmosphere or using ethanol as a solvent in staining solutions. *RNA* **14**, 2698–2704 (2008).
36. Chomczynski, P. & Sacchi, N. The single-step method of RNA isolation by acid guanidinium thiocyanate-phenol-chloroform extraction: twenty-something years on. *Nat. Protoc.* **1**, 581–585 (2006).
37. Bengtsson, M., Hemberg, M., Rorsman, P. & Stahlberg, A. Quantification of mRNA in single cells and modelling of RT-qPCR induced noise. *BMC Mol. Biol.* **9**, 63 (2008).
38. Trombetta, J.J. *et al.* Preparation of single-cell RNA-seq libraries for next generation sequencing. *Curr. Protoc. Mol. Biol.* **107**, 4.22.1–4.22.17 (2014).
39. Miller, D.F. *et al.* A new method for stranded whole transcriptome RNA-seq. *Methods* **63**, 126–134 (2013).
40. Achim, K. *et al.* High-throughput spatial mapping of single-cell RNA-seq data to tissue of origin. *Nat. Biotechnol.* **33**, 503–509 (2015).
41. Satija, R., Farrell, J.A., Gennert, D., Schier, A.F. & Regev, A. Spatial reconstruction of single-cell gene expression data. *Nat. Biotechnol.* **33**, 495–502 (2015).
42. Durruthy-Durruthy, R., Gottlieb, A. & Heller, S. 3D computational reconstruction of tissues with hollow spherical morphologies using single-cell gene expression data. *Nat. Protoc.* **10**, 459–474 (2015).
43. Junker, J.P. *et al.* Genome-wide RNA tomography in the zebrafish embryo. *Cell* **159**, 662–675 (2014).
44. Kim, D. *et al.* TopHat2: accurate alignment of transcriptomes in the presence of insertions, deletions and gene fusions. *Genome Biol.* **14**, R36 (2013).
45. Trapnell, C. *et al.* Differential gene and transcript expression analysis of RNA-seq experiments with TopHat and Cufflinks. *Nat. Protoc.* **7**, 562–578 (2012).
46. Huber, W., von Heydebreck, A., Sultmann, H., Poustka, A. & Vingron, M. Variance stabilization applied to microarray data calibration and to the quantification of differential expression. *Bioinformatics* **18**, S96–104 (2002).
47. Zhang, W. *et al.* Integrating genomic, epigenomic, and transcriptomic features reveals modular signatures underlying poor prognosis in ovarian cancer. *Cell Rep.* **4**, 542–553 (2013).

Corrigendum: Spatial transcriptomic analysis of cryosectioned tissue samples with Geo-seq

Jun Chen, Shengbao Suo, Patrick PL Tam, Jing-Dong J Han, Guangdun Peng & Naihe Jing

Nat. Protoc. **12**, 566–580 (2017); published online 16 February 2017; corrected after print 13 April 2017

In the version of this article initially published, Shengbao Suo was not indicated as contributing equally to the work with Jun Chen; Jing-Dong J. Han was not indicated as a corresponding author; the expanded form of "Geo-seq" was not given in the abstract; in the heading prior to Step 77, it was not stated that the time indicated excludes the time required for the design of 2D corn plots and for zip-code mapping; "Corn plot visualization and zip-code mapping can be performed through the iTranscriptome portal at http://www.itranscriptome.org." was omitted from the end of Step 77; and some grant numbers were omitted from the Acknowledgments section. These omissions have been corrected in the HTML and PDF versions of the article.